Penerbit Akademia Baru

Journal of Advanced Research in Fluid Mechanics and Thermal Sciences

Journal homepage: www.akademiabaru.com/arfmts.html
ISSN: 2289-7879

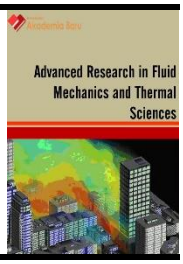

Aerodynamic Drag Study of Time-Trial Cycling Helmets Using CFD Analysis

Open Access

Mohd Salahuddin Mohd Basri[1,2,*], Khairul Manami Kamarudin[3], Nurul Ain Maidin[4], Mohd Hidayat Ab Rahman[4]

[1] Department of Process and Food Engineering, Faculty of Engineering, University Putra Malaysia, 43400 UPM Serdang, Selangor, Malaysia
[2] Laboratory of Halal Science Research, Halal Products Research Institute, Universiti Putra Malaysia, 43400 Serdang, Malaysia
[3] Department of Industrial Design, Faculty of Design and Architecture, University Putra Malaysia, 43400 UPM Serdang, Selangor, Malaysia
[4] Faculty of Mechanical and Manufacturing Engineering Technology, Universiti Teknikal Malaysia Melaka, Hang Tuah Jaya, 76100 Durian Tunggal, Melaka, Malaysia

ARTICLE INFO

Article history:
Received 26 December 2019
Received in revised form 27 March 2020
Accepted 27 March 2020
Available online 8 June 2020

ABSTRACT

In cycling events, aerodynamic drag contributes most of the resistance experienced by a competitive cyclist. Accordingly, the majority of time-trial cycling helmets were designed to obtain low aerodynamic drag. The question arises what is the best position of cycling helmet and its tail flap that resulted in the lowest drag coefficient. This paper presents an aerodynamic drag analysis of helmet with different tail flap positions at a constant speed of 60 km per hour. The objective of this paper was to investigate the drag coefficient between the different designs of helmet and tail flips using CFD and thoroughly study the airflow near the surface of the cyclist helmet. The results are compared with the exceptional time trial cycling helmet in the market. Design of a 2D-model of cycling helmets is developed using GAMBIT software. Six helmet designs comprising varying tail flap positions were tested under ideal cycling position. The designs are the existing time trial cycling helmet available in the market (Helmet 1), the modified helmets with tail flap at 0, 3, 6 and 9 degrees to horizontal (Helmet 2 to 5) and the modified 10 degrees rotated helmet (Helmet 6). The computational fluid dynamics simulations are performed using ANSYS Fluent and the results in terms of the reduced drag coefficient and flow characteristics for optimal aerodynamic performance are analyzed. It is shown that the tail flap position of 6 and 9 degree to horizontal produce considerably low drag coefficient with 0.06 and 0.05, respectively, while the modified 10 degree rotated helmet recorded the highest drag coefficient due to large frontal area and flow separation. Evidently, closer tail flap to the back of the cyclist and smaller pressure difference resulted in the low drag coefficient.

Keywords:
Aerodynamic drag; time-trial; cycling helmet; CFD analysis; fluid flow

[*] *Corresponding author.*
E-mail address: salahuddin@upm.edu.my (Mohd Salahuddin Mohd Basri)

https://doi.org/10.37934/arfmts.72.1.2131

1. Introduction

Time is the critical factor when cycling against the clock in a time trial or triathlon. Lower time taken leads to a better potential result. According to Bradford and Jenkins [1], a cyclist travelling at 20 mph on flat terrain experienced more than 80 percent resistance which is contributed by aerodynamic drag. When a cyclist or tri-athletes reaches speeds of more than 30 mph, low aerodynamic drag is a key quality of high-performance cycling. Barelle [2] studied drag resistance on three different positions; i.e., high, usual (normal) or low inclination of the head in the time trial. The result shows that the drag resistance for the usual inclination was the lowest indicating the best position with 37.2 N. The results for low and high inclinations were 37.8 N and 38.5 N, respectively. She concluded that helmet shape and inclination of the head can have different impacts on the projected frontal area of the athlete´s head and thus on aerodynamic drag.

Investigation on 14 time-trial helmets was conducted by Blair and Sidelko [3] to identify the effect of different yaw angles on the drag coefficient and performance. They found that the well-performing helmets were able to reduce the drag up to 10 percent as compared to that of the poorly performing helmets. Helmet with extreme high inclination angles produced an overall high drag. However, the relationship between helmet design and performance was not conducted.

Since the type of boundary layer and its thickness influence the surface friction drag and any flow separation, it is important to know that the layer is strongly influenced by how the pressure varies along the direction of flow. Other important factors are speed, density and viscosity of the air; also, for a given geometric shape, the size of the helmet is important. If the Reynolds number is increased by increasing the speed of the cyclist, the transition position moves forward, and the boundary layer becomes thinner [4]. It can, therefore, be seen that the value of the Reynolds number is important in determining the type of flow around the helmet.

When air flows over the top of a surface, the pressure then gradually rises again as the flow speed decreases. This means that the air has to travel from a low to a high pressure, which it can do by slowing down and losing some of its kinetic energy. The situation can be likened to that of a cyclist coasting up a hill, which is possible as long as it is travelling fast enough at the bottom [5]. If the increase in pressure is gradual, the process of turbulent mixing allows the outer layers to effectively pull the inner ones along. If the rate of increase of pressure is too high, however, the mixing process will be too slow to keep the lower part of the layer moving. When this happens, the boundary layer flow stops following the contours of the surface and separates away [6]. Air particles downstream of the separation position tend to move towards the lower pressure in the reverse direction to the main flow. Besides, surface structure and flow separation affect the drag coefficient. Reseach conducted by Dandan *et al.,* found that the outward dimple surface caused the flow separation to delay, resulting in low drag coefficient [7].

Besides empirical investigations, numerical modelling such as computational fluid dynamic (CFD) is an effective tool to simulate complex fluid flows [8]. Numerous studies have been conducted using CFD method to investigate the aerodynamic drag of cyclists and improve the aerodynamic design of the bicycle helmet [1]. Blocken *et al.,* studied the aerodynamic drag of two drafting cyclists using CFD simulation and found that the drag reductions decrease when the distance between both cyclists increased [9]. Defraeye *et al.,* investigated the accuracy of CFD simulation by comparing with full-scale wind-tunnel tests for different cyclist positions. They found that the CFD simulation is a comparably accurate tool to study the drag of different cyclist positions and to investigate the influence of small adjustments in the cyclist's position [10]. Defraeye *et al.,* (2011) continued in investigating drag and convective heat transfer for cyclists at a high spatial resolution. They concluded that high drag values were recorded for the head, legs and arms [11]. However, to our

knowledge, limited numerical studies have been performed on the aerodynamic performance of a modified helmet with tail flip and discuss in detail the airflow within the boundary layer. Therefore, the objective of this paper was to investigate the drag coefficient between the different designs of helmet and tail flips using CFD and thoroughly study the airflow near the surface of the cyclist helmet.

2. Methodology

2.1 Geometry, Computational Domain and Boundary Conditions

To assess the effect of helmet shape on aerodynamic performance, a total of six different design of the time-trial cycling helmets were selected for this study. Helmet 1 is referred to as existing time-trial cycling helmet in the market. For anonymity, the brand name and the manufacturer of the helmets we not identified in this study. Helmet 2, Helmet 3, Helmet 4 and Helmet 5 are referred to as a modified helmet with a tail flap of 0, 3, 6, 9 degrees to the horizontal, respectively as shown in Figure 1. Helmet 6 is referred to as a modified helmet rotated 10 degrees counter-clockwise with a tail flap placed close to the back of the cyclist.

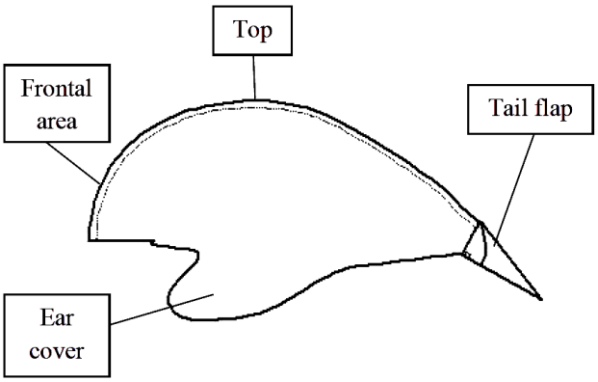

Fig. 1. Modified aerodynamic helmet with tail flap

The helmets were numbered as Helmet 1 to 6 as shown in Figure 2. All helmets were modelled in GAMBIT based on the ideal cycling position of the cyclist which the helmet tip was very close to the back of the cyclist.

For this computational fluid dynamics analysis, the geometry and the computational and fluid domain considered was 15 metres in length and 6 metres in height according to the best practice guidelines as shown in Figure 3 [12]. The helmet was positioned at 5 metres from the inlet of the domain. Only the upper part of the helmet and the back of the cyclist were modelled since the research is focusing on analyzing the airflow at these areas and the computation time will be minimized [9]. The finer mesh was constructed near the helmet surfaces and it was biased towards boundary walls. Quadrilateral elements were used to discretise the flow domain volume. Tetrahedral elements were built at the area under the tip of the helmet.

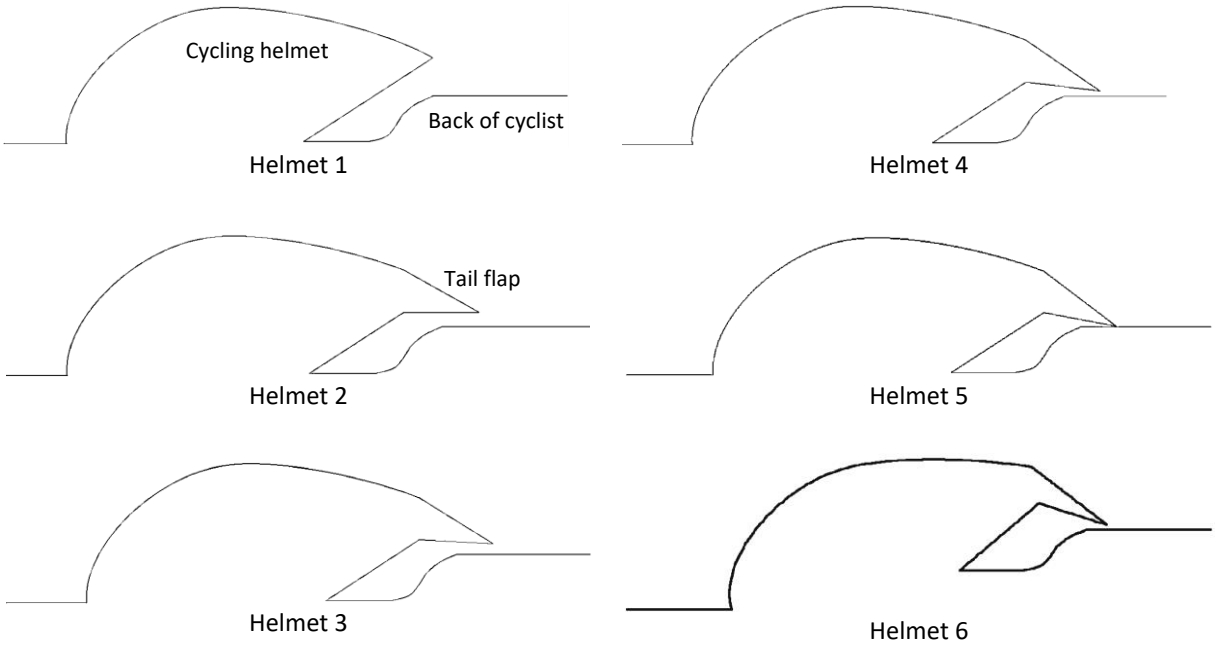

Fig. 2. 2-D models of different tip design and position of time-trial cycling helmets

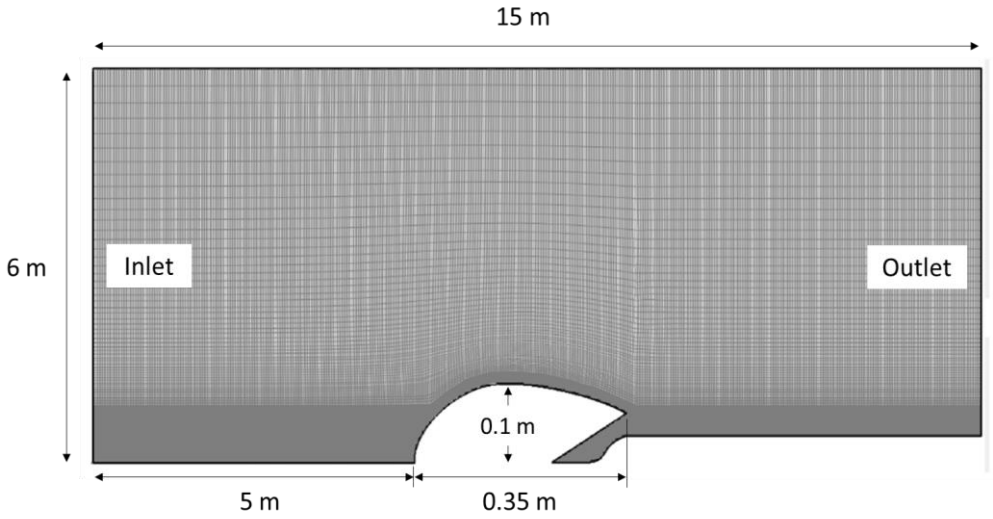

Fig. 3. Computational mesh and domain of the CFD analysis

The model was imported to ANSYS Fluent where boundary conditions were applied. At the inlet velocity condition, a uniform constant horizontal velocity of 16.7 m/s was imposed. This condition is based on the time recorded in the time-trial competition for an elite cyclist which is between 50 to 60 km/h [13]. The speed of 57 to 60 km/h was mentioned to be the average speed for a winning time [14]. At the outlet, pressure conditions with ambient static pressure were applied.

2.2 Mesh and Drag Coefficient

Three models with different mesh densities were created. Coarse, medium and fine mesh densities were compared. The number of cells for coarse, medium and fine mesh were 43121, 96441 and 185903, respectively. Referring to Ouakka and Fantuzzi [15], the mesh density for coarse mesh was decided to be reduced by half of the medium mesh and for fine mesh, the mesh density was

doubled from the medium mesh. To determine which type of mesh was optimal for further simulation, the values of drag coefficient were compared and the percent difference calculated. Taking the medium mesh density as the benchmark, the difference in drag coefficient with fine mesh is relatively small which is 5.3 percent as compared to that of the difference with coarse mesh which is 26.3 percent. Medium-density mesh was considered optimal in providing sufficient resolution for drag coefficient analysis.

The drag coefficient (C_D) is mainly dependent on the shape of the helmet. In addition to this shape-related coefficient, the aerodynamic drag also depends on the frontal area of the helmet, the air density and the square of the relative air speed. The relationship between drag coefficient and these factors can be expressed by Eq. (1) where F_D is the aerodynamic drag, A is the frontal area, ρ_∞ is the density of the air, and V_∞ is the speed of the cyclist relative to the air [16].

$$C_D = \frac{2 \cdot F_D}{A \cdot \rho_\infty \cdot {V_\infty}^2} \quad (1)$$

2.3 CFD Simulation

Simulations were performed using ANSYS Fluent 17. The turbulence model is used based on Reynold's Number calculated, which was 400141, and in accordance to other researches which yield reasonable results including in swimming and cycling studies [9,17,18]. The turbulence model used was a Standard K-epsilon model which determined the turbulent length and time scale by solving two separate model transport equations for the turbulence kinetic energy (k) and dissipation rate (ε). The second-order discretization schemes were used to limit numerical dissipation. Standard wall functions were selected for the near-wall treatment of turbulence and the turbulence intensity at the entry of the field was set at one percent. During computations, the criterion of convergence of 10^{-5} was set following previous literature [19].

3. Results

3.1 Modelling Validation

The helmet used in previous literature reported by Alam *et al*., [20], with all the venting holes covered, was used as control. The numerical procedure was validated by comparing with experimental and computational data. The drag coefficient (C_D) reported for the helmet is 0.21. For validation purposes, the design of the helmet was produced using GAMBIT software and exported to ANSYS Fluent for simulation. The drag coefficient recorded after the CFD simulation is approximately 0.19. The difference compared to the literature was approximately 9 percent due mainly to dissimilarity in the computational domain. Our results are close to the result deduced from Alam *et al*., [20] and the CFD simulation used is acceptable.

3.2 Analysis of Flow Patterns

In time-trial cycling competition, air flowing over the cycling helmet contributed to overall aerodynamics and has a huge impact on the overall performance of the cyclist. Formation of boundary layer around the helmet when it was exposed to the airflow can be changed by modifying the shape or design of the helmet. The streamline patterns, coloured by velocity, for Helmet 1, 2 and 3 are shown in Figure 4(a)-(c) and analyzed in detail.

In Figure 4(a), laminar flow formed at the front part of the helmet (point A). As the flow travelled further, laminar separation bubbles occurred at point B due to a strong adverse pressure gradient

(pressure changes along the surface), which forced the laminar boundary layer to separate from the curved helmet surface. At point C, the separation reattached to the helmet surface before the layer separated again and formed a vortex at point D. As the flow passed the tip of the helmet, turbulence formed with a large separation at point E. The vortex formed at this point slowly disappeared. High drag coefficient value was expected due to the large separation as mentioned by Bearman and Morel [21].

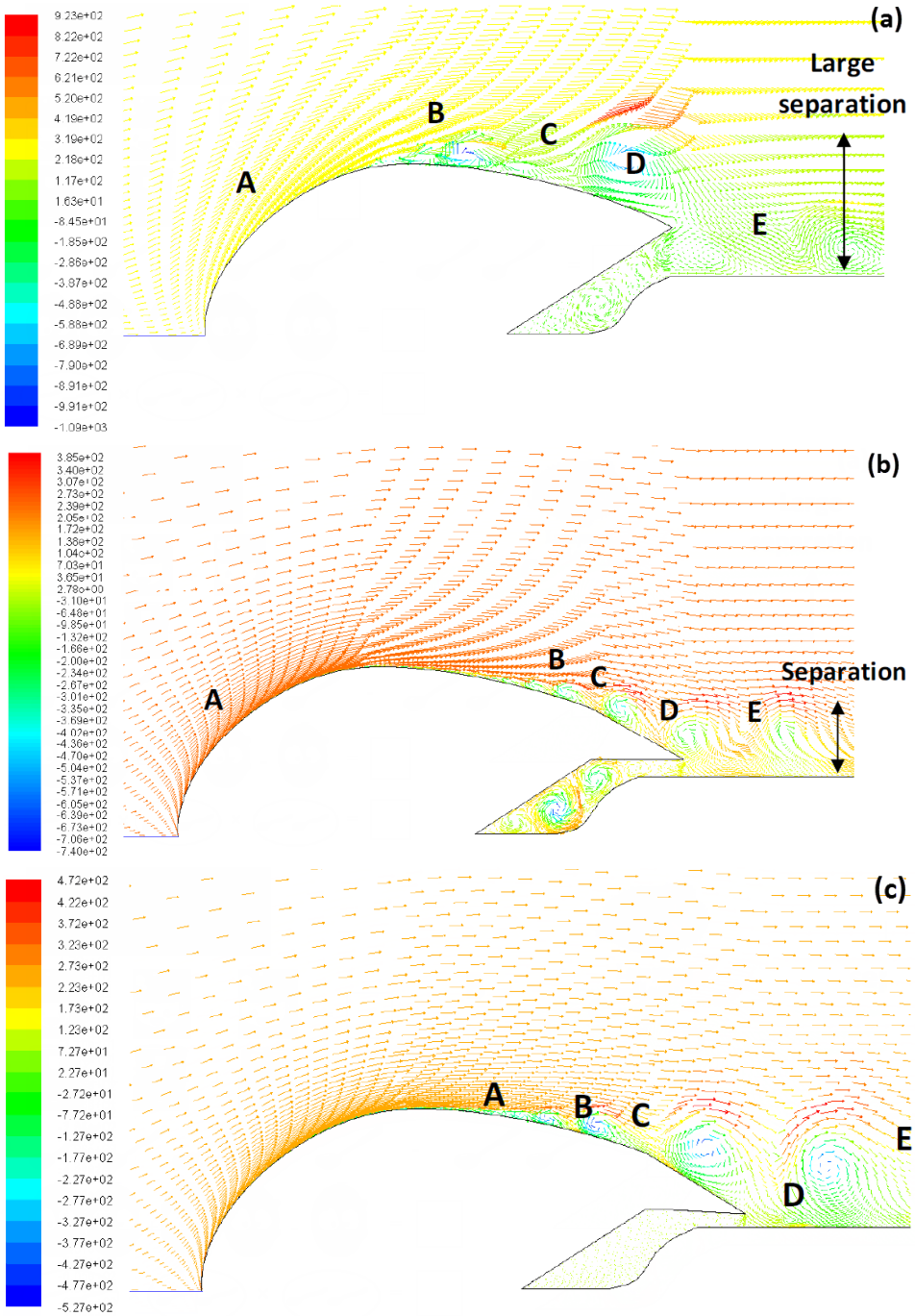

Fig. 4. Streamline patterns colored by velocity for (a) Helmet 1, (b) Helmet 2, and (c) Helmet 3

In Figure 4(b), laminar flow occurred at the front part of the helmet (point A). Bubble separation at point B formed a little further from the frontal area as compared to Helmet 1. The separation was

highly sensitive to disturbances. Thus, the flow reattached at point C and quickly formed a vortex at point D, very close to the surface, and producing more drag. As the flow travelled further, it reattached again and quickly forms more vortices with a considerable large separation at the tip of the helmet. Trailing vortex as well as high pressure formed at point E. The high drag coefficient obtained probably due to the high-pressure area.

At three degrees flap as shown in Figure 4(c), the separation occurred at point A further back from helmet face relative to that for Helmet 1 and 2. The flow however quickly reattached at point B and just as rapidly formed a vortex at point C. In this transition zone, the vortex attached closely to the surface and later reattached under low pressure at point D. Another low-pressure vortex formed beyond this (point E) but did not attach to the surface and was quickly shed. The total drag coefficient was lower compared to Helmet 2 because most of the low pressures were formed within the boundary layer in the transition and turbulent flow regions.

At point A in Figure 5(a), the laminar flow formed much earlier as in Helmet 1 and 2. As the flow travelled further to the back, it enters the transition region where a laminar separation bubble formed at point B.

As the thickness of the bubble grew, a vortex appeared at point C. The flow reattached at point D and produced high pressure at the tip of the helmet. Immediately the flow to the rear formed a vortex not closely attached to the surface (point E) and where it quickly formed another vortex. The trailing vortices however quickly disappeared.

In Figure 5(b), the tip of the helmet was placed exactly on the back of the cyclist. Laminar separation bubble appeared at point A. Inside the bubble, the flow was circular in the opposite direction to the outer flow at the surface. As the bubble thickened, it rapidly became turbulent generating a small vortex at point B. A low-pressure vortex than formed at point C but quickly reattached to the surface. The flow was quite similar to that in Helmet 4 except that the separation bubble formed was smaller and the vortices shed much quicker thus resulting in the lowest drag coefficient (0.05) of all the tested helmets.

During the competition, the cyclist cannot maintain his or her head at the optimal angle. When the cyclist rotated the helmet 10 degrees (yaw angle to the horizontal) counter-clockwise, the tail flap tended to move close to the cyclist´s back. At this position, a frontal area larger than usual would form resulting in higher drag coefficient as shown in Figure 5(c). This position also created higher total force (pressure and viscous force). Since total force is directly proportional to the drag coefficient, an increase in total force will increase in the drag coefficient. There was a very small separation bubble formed at point B. However, as the flow entered point C, sudden changes in velocity and pressure created a turbulent flow with a trailing vortex at point D. Higher drag coefficients (0.16) obtained relative to other cases were most probably due to the larger frontal area and large flow separation. This result agrees with one reported by Zdravkovich *et al.*, [22]. Drag coefficients for all helmet are summarized in Table 1.

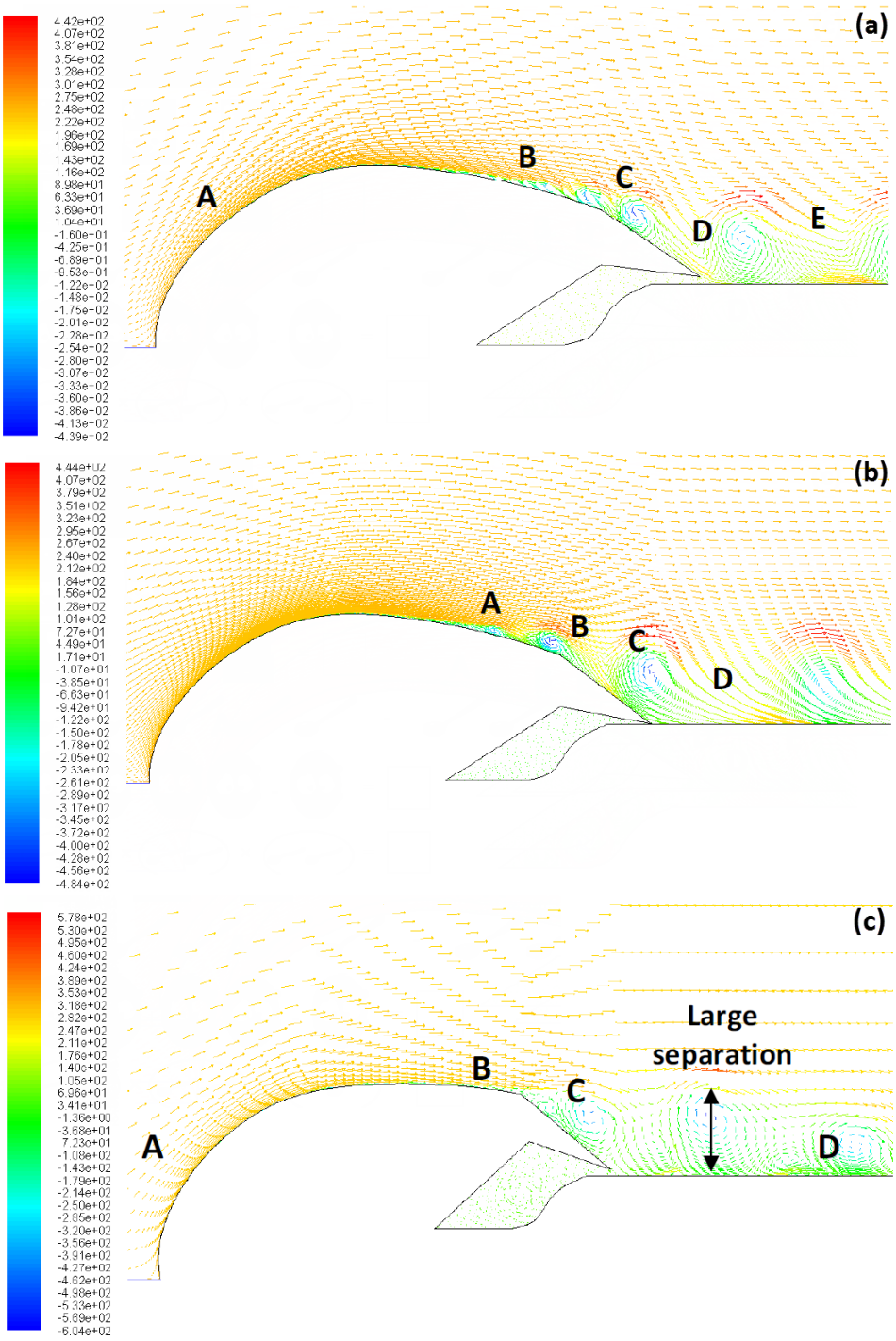

Fig. 5. Streamline patterns colored by velocity for (a) Helmet 4, (b) Helmet 5, and (c) Helmet 6

Table 1
The drag coefficient for six helmets

Helmet	1	2	3	4	5	6
Drag coefficient (C_D)	0.19	0.10	0.09	0.06	0.05	0.16

3.3 Analysis of the Pressure Field

According to Gibertini and Grassi [23], the largest proportion to the aerodynamic resistance is mainly from pressure drag. As air flows around the helmet, the local pressure and velocity change. An increase in the local pressure resulted in faster movement of gas molecules at all directions, thus creating forces. The gas molecules that move at the opposite direction to the airflow, which created forces against the airflow, was called drag. Graph pressure versus position point on the helmet for each case was analyzed to show the relationship between pressures and drag as shown in Figure 6(a)-(f). It can be seen that a stagnation pressure appeared in most of the graphs and showed by a straight line between the position of 0.1 and 0.25m. The stagnation pressure appeared due to a viscous interaction between the free stream and the stagnating fluid. Higher stagnation pressure caused by higher amount of energy transferred between the free stream and the stagnating fluid [24]. The air velocity at the stagnation pressure point is equal to zero and the pressure recorded is calculated by the total pressure points [25].

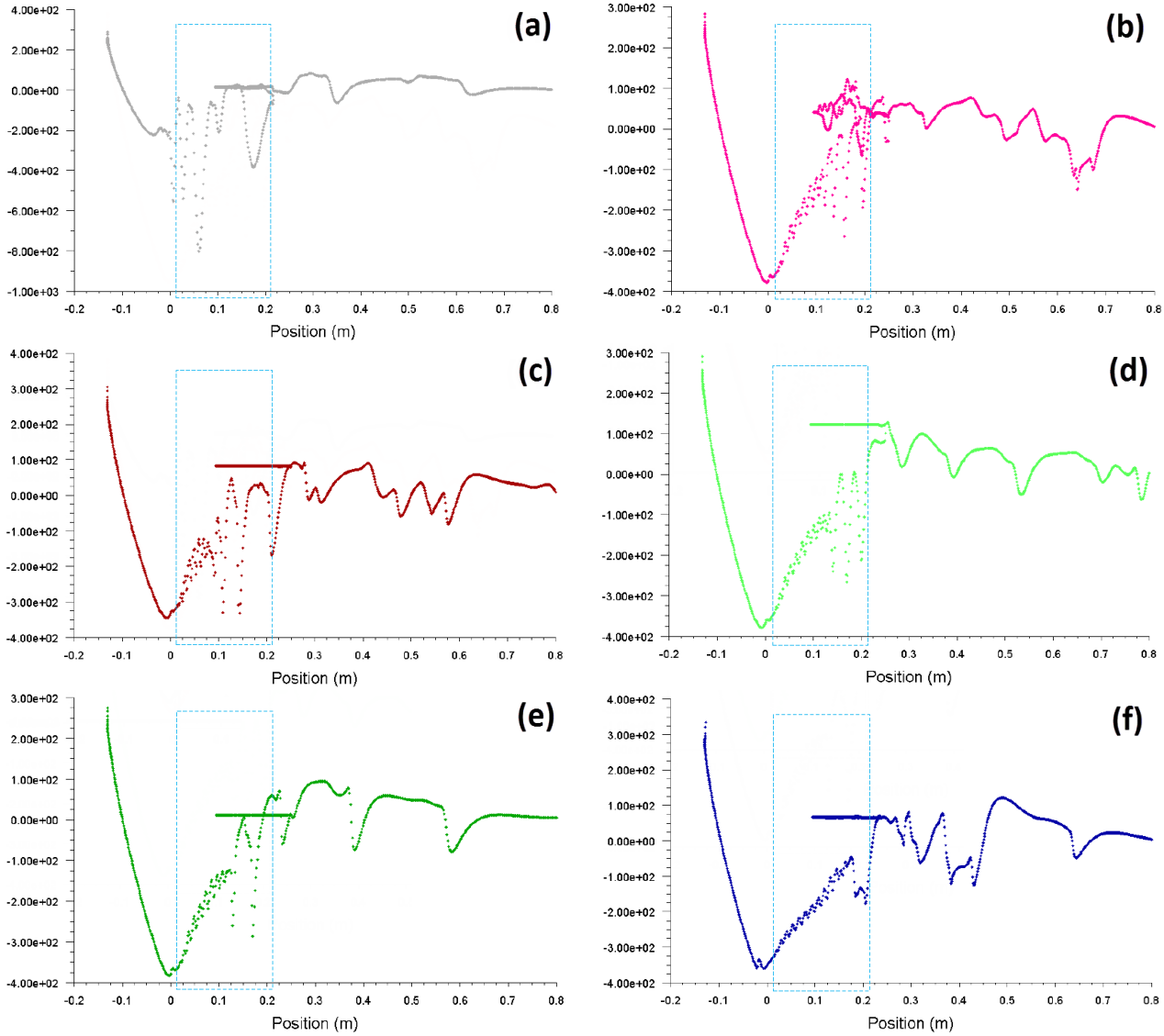

Fig. 6. Pressure on (a) Helmet 1, (b) Helmet 2, (c) Helmet 3, (d) Helmet 4, (e) Helmet 5, (f) Helmet 6

Rapid and persistent changes in pressure will easily form separation bubbles, vortices and turbulent flow. In Figure 6(a), the pressure difference between the highest and lowest pressure was approximately 0.8 MPa for Helmet 1 at the position of 0 to 0.2 m. This zone of pressure difference was located from middle to the tip of the helmet. The pressure difference recorded for Helmet 1 was much higher as compared to that of other helmets which were between 0.4 and 0.5 MPa. This zone of pressure difference was located from middle to the tip of the helmet. For Helmet 2 to 5 in Figure 6(b-e), respectively, graph fluctuations within the 0 to 0.2 m zone were higher in Helmet 2, decreasing gradually until Helmet 5. Greater graph fluctuation indicates more pressure changes which bear influence on the value of drag coefficient. For Helmet 6 in Figure 6(f), pressure changes in similar zone range were the smallest. However, higher pressure formed at the frontal area of the helmet indicated higher drag occurrence. In this way, the frontal area can greatly affect the value of the drag coefficient.

4. Conclusions

This study aims to investigate the drag coefficient and flow behavior for different designs of helmet and tail flips using CFD analysis. The cycling helmet with the tail flap position of 6 and 9 degree to horizontal, which is very close to the back of the cyclist, produce considerably low drag coefficient while the modified 10 degree rotated helmet recorded the highest drag coefficient (0.16) due to large frontal area and flow separation. Formation of vortices, trailing vortices, laminar separation bubbles, turbulent flow, and separation at the tip of the tail flap was recorded in all designs. However, the amount of pressure drags, size and position of the streamline flow significantly determine the value of the drag coefficient.

Acknowledgement
The authors would like to thank the Universiti Putra Malaysia for laboratory facilities.

References
[1] Sims, Bradford W., and Peter E. Jenkins. "Aerodynamic bicycle helmet design using a truncated airfoil with trailing edge modifications." In *ASME 2011 International Mechanical Engineering Congress and Exposition*, pp. 453-462. American Society of Mechanical Engineers Digital Collection, 2011. https://doi.org/10.1115/IMECE2011-65411

[2] Barelle, Caroline. "Sport Aerodynamics: on the Relevance of Aerodynamic Force Modelling versus Wind Tunnel Testing." *Wind Tunnels and Experimental Fluid Dynamics Research* (2011): 349-368. https://doi.org/10.5772/21586

[3] Blair, Kim B., and Stephanie Sidelko. "Aerodynamic performance of cycling time trial helmets (p76)." *The Engineering of Sport 7* (2008): 371-377. https://doi.org/10.1007/978-2-287-09411-8_44

[4] Barnard, Richard Harry. *Road vehicle aerodynamic design-an introduction*. 2001.

[5] Crouch, Timothy N., David Burton, Zach A. LaBry, and Kim B. Blair. "Riding against the wind: a review of competition cycling aerodynamics." *Sports Engineering* 20, no. 2 (2017): 81-110. https://doi.org/10.1007/s12283-017-0234-1

[6] Stager, Joel M., and David A. Tanner, eds. *The Handbook of Sports Medicine and Science: Swimming*. John Wiley & Sons, 2008.

[7] Dandan, Muhammad Arif, Syahrullail Samion, Mohamad Nor Musa, and Fazila M. Zawawi. "Evaluation of Lift and Drag Force of Outward Dimple Cylinder Using Wind Tunnel." *CFD Letters* 11, no. 3 (2019): 145-153. http://www.akademiabaru.com/doc/CFDLV11_N3_P145_153.pdf

[8] Gardan, N., Alexandre Schneider, G. Polidori, H. Trenchard, Jean-Marc Seigneur, F. Beaumont, F. Fourchet, and R. Taiar. "Numerical investigation of the early flight phase in ski-jumping." *Journal of biomechanics* 59 (2017): 29-34. https://doi.org/10.1016/j.jbiomech.2017.05.013

[9] Blocken, Bert, Thijs Defraeye, Erwin Koninckx, Jan Carmeliet, and Peter Hespel. "CFD simulations of the aerodynamic drag of two drafting cyclists." *Computers & Fluids* 71 (2013): 435-445. https://doi.org/10.1016/j.compfluid.2012.11.012

[10] Defraeye, Thijs, Bert Blocken, Erwin Koninckx, Peter Hespel, and Jan Carmeliet. "Aerodynamic study of different cyclist positions: CFD analysis and full-scale wind-tunnel tests." *Journal of biomechanics* 43, no. 7 (2010): 1262-1268. https://doi.org/10.1016/j.jbiomech.2010.01.025

[11] Defraeye, Thijs, Bert Blocken, Erwin Koninckx, Peter Hespel, and Jan Carmeliet. "Computational fluid dynamics analysis of drag and convective heat transfer of individual body segments for different cyclist positions." *Journal of biomechanics* 44, no. 9 (2011): 1695-1701. https://doi.org/10.1016/j.jbiomech.2011.03.035

[12] Giappino, S., S. Omarini, P. Schito, S. Somaschini, M. Belloli, and M. Tenni. "Cyclist aerodynamics: a comparison between wind tunnel tests and CFD simulations for helmet design." In *Conference of the Italian Association for Wind Engineering*, pp. 336-349. Springer, Cham, 2018. https://doi.org/10.1007/978-3-030-12815-9_27

[13] Burke, Ed. *High-tech cycling*. Human Kinetics, 2003.

[14] Broker, J.P., Kyle, C.R. and Burke, E.R. "Racing cyclist power requirements in the 4000-m individual and team pursuits." *Medicine & Science in Sports & Exercise* 31, no. 11 (1999): 1677. https://doi.org/10.1097/00005768-199911000-00026

[15] Ouakka, Slimane, and Nicholas Fantuzzi. "Trustworthiness in Modeling Unreinforced and Reinforced T-Joints with Finite Elements." *Mathematical and Computational Applications* 24, no. 1 (2019): 27. https://doi.org/10.3390/mca24010027

[16] Wahba, E. M., Humaid Al-Marzooqi, Majd Shaath, Mohamed Shahin, and Tarek El-Dhmashawy. "Aerodynamic Drag Reduction for Ground Vehicles using Lateral Guide Vanes." *CFD Letters* 4, no. 2 (2012): 68-79. http://www.akademiabaru.com/doc/CFDLV4_N2_P68_79.pdf

[17] Zaidi, Hanane, Stephane Fohanno, Redha Taiar, and Guillaume Polidori. "Turbulence model choice for the calculation of drag forces when using the CFD method." *Journal of biomechanics* 43, no. 3 (2010): 405-411. https://doi.org/10.1016/j.jbiomech.2009.10.010

[18] Fintelman, D. M., Mark Sterling, Hassan Hemida, and F-X. Li. "The effect of crosswinds on cyclists: an experimental study." *Procedia Engineering* 72 (2014): 720-725. https://doi.org/10.1016/j.proeng.2014.06.122

[19] Zaidi, H., R. Taiar, S. Fohanno, and G. Polidori. "Analysis of the effect of swimmer's head position on swimming performance using computational fluid dynamics." *Journal of Biomechanics* 41, no. 6 (2008): 1350-1358. https://doi.org/10.1016/j.jbiomech.2008.02.005

[20] Alam, Firoz, Simon Watkins, and Aleksandar Subic. "Aerodynamic efficiency and thermal comfort of bicycle helmets." In *Proc. of the 6th International Conference on Mechanical Engineering (ICME2005), TH-32 (1-6)*, pp. 28-30. 2005.

[21] Bearman, P. W., and T. Morel. "Effect of free stream turbulence on the flow around bluff bodies." *Progress in aerospace sciences* 20, no. 2-3 (1983): 97-123. https://doi.org/10.1016/0376-0421(83)90002-7

[22] Zdravkovich, M. M., M. W. Ashcroft, S. J. Chisholm, and N. Hicks. "Effect of cyclist's posture and vicinity of another cyclist on aerodynamic drag." *The engineering of sport* 1 (1996): 21-28.

[23] Gibertini, Giuseppe, and Donato Grassi. "Cycling aerodynamics." In *Sport aerodynamics*, pp. 23-47. Springer, Vienna, 2008. https://doi.org/10.1007/978-3-211-89297-8_3

[24] Kim, K. "Pneumatic Measurements for Pressure, Velocity, and Flow-direction." In *Application of Thermo-Fluidic Measurement Techniques*, pp. 61-100. Butterworth-Heinemann, 2016. https://doi.org/10.1016/B978-0-12-809731-1.00003-4

[25] Goodfellow, Howard D. *Industrial ventilation design guidebook*. Elsevier, 2001.